Available online at www.sciencedirect.com
ScienceDirect
Journal of Nuclear Materials 360 (2007) 118–127
journal of nuclear materials
www.elsevier.com/locate/jnucmat

Interatomic potentials consistent with thermodynamics: The Fe–Cu system

R.C. Pasianot [a,b], L. Malerba [c,*]

[a] Departamento de Materiales, CAC-CNEA, Avda. Gral. Paz 1499, 1650 San Martín, Pcia. Buenos Aires, Argentina
[b] CONICET, Avda. Rivadavia 1917, 1033 Buenos Aires, Argentina
[c] Reactor Materials Research Unit, SCK-CEN, Boeretang 200, B-2400 Mol, Belgium

Received 4 July 2006; accepted 22 September 2006

Abstract

A methodology is developed to fit semi-empirical interatomic potentials aimed at obtaining a consistent thermodynamic behavior. The procedure is based on the cluster variation method theory which is seamlessly integrated to the other more standard equations of the fitting technique. A new interatomic potential for the Fe–Cu system is thus built within the framework of the embedded atom method, to be used in studies of the microstructure evolution of Fe–Cu alloys under irradiation. The potential is shown to reproduce very reasonably the Cu solubility curve in the Fe matrix as well as to lead to better description of the point defect kinetics with respect to previous interaction models. Limitations of the fitting technique and possible ways of improvement are discussed.

PACS: 61.80.Az; 61.82.Bg; 61.72.Bb; 31.15.Qg

1. Introduction

Interatomic potentials are the core of atomistic computer simulations and determine the degree of reliability of the results obtained from this type of models. The atomic level mechanisms and phenomena simulated using molecular dynamics (MD) or atomistic kinetic Monte Carlo (MC) (Table 1) techniques can only be considered representative of the real material behavior if the potential reflects correctly the properties of relevance for the problem at hand. In radiation damage studies, clearly the most important of these properties are point defect energies and configurations. Also desirable are energies and configurations of more extended defects, such as clusters, dislocations, stacking faults and grain boundaries. In the case of alloys, however, the microstructural evolution under irradiation is decided by the interplay between defect formation and migration and thermodynamic driving forces, together determining the appearance or not of certain phase transformations (precipitation, segregation, etc.). It is therefore very desirable that an interatomic potential reproduces as closely as possible the stability of the phases that can appear at least in the concentration range of interest.

* Corresponding author. Tel.: +32 0 14 333090; fax: +32 0 14 321216.
E-mail address: lmalerba@sckcen.be (L. Malerba).

0022-3115/$ - see front matter © 2006 Elsevier B.V. All rights reserved.
doi:10.1016/j.jnucmat.2006.09.008

Table 1
List of acronyms used throughout the article

Acronym	Meaning
AB	Ackland-Bacon potential
AKMC	Atomistic kinetic Monte Carlo
ATAT	Alloy theoretic automated toolkit
CO5.20	Present Fe–Cu potential
CVM	Cluster variation method
EAM	Embedded atom method
LF	Ludwig–Farkas potential
MC	Monte Carlo
MD	Molecular dynamics
MMC	Metropolis Monte Carlo
OF	Objective function
RPV	Reactor pressure vessel
1 nn, 2 nn, ...	1st, 2nd, ... nearest neighbor

To date, cross potentials for binary alloys are mainly fitted to a limited number of alloy parameters, such as heat of solution, mixing enthalpy of liquid mixtures, ordered compound energies, point defect binding energies, etc. [1–6]. It is only by chance that these procedures can guarantee the capability of the potential to fulfill the aforementioned thermodynamic requirements. To improve this situation the idea is therefore to use phase diagram points as reference data for the fabrication of an alloy potential, in addition to the usual set of fitting data, such as elastic constants, cohesive energies, lattice parameter, defect formation energies, etc. In order to do this, however, one must devise a formalism to express the thermodynamic functions of the alloy versus the fitting parameters of the potential. These can then in principle be adjusted in such a way that the thermodynamic functions are correctly reproduced. For the opposite route, namely, given the cohesive model (e.g. an interatomic potential) to compute the free energies, there are well known methods based on MD and/or MC techniques able to perform the task for any aggregation state (see e.g. Chap. 7 et seq. of Frenkel and Smit's book [7]), thus the complete phase diagram can be derived. Though these methods can also be applied to multicomponent mixtures [8], concrete examples in the literature are rather scarce. Among the few of them, full phase diagrams computed from available alloy potentials have been reported for the Au–Ni [9] and Fe–Cu [10] systems. However, due to the complexity and variety of the calculations involved, the inversion of these methods appears in general unfeasible.

More specific techniques are available for the less ambitious task of computing only the solid part of the phase diagram. These methods [11] are mainly based on the Ising spin-like Hamiltonian to express the energy and subsequent application of statistical mechanics techniques such as MC, low and high temperature expansions, etc., to allow for the entropy contribution. Among these the so called cluster variation method (CVM), introduced by Kikuchi in 1951 [12], has been successfully applied to a wide variety of systems [13]. Though being a mean-field technique, CVM can be as accurate as the heavier MC techniques (except near critical lines or points) and possesses the distinctive feature of providing analytic expressions for the (configurational) entropy. The use of the Ising formalism to express the energy, coupled with the CVM to express the entropy, appears therefore attractive and manageable also to follow the opposite path of fitting a cohesive model to a given phase diagram.

The methodology hinted at above is here applied to fabricate a new Fe–Cu potential, meant for the study of Cu precipitation in Fe under irradiation. The choice of this system is due to a number of considerations.

Firstly, the very low solubility of Cu in Fe is the main driving force for the appearance of Cu-rich precipitates in reactor pressure vessel (RPV) steels subjected to neutron irradiation during operation; such microstructural features are among the main causes of embrittlement of these steels [14–18]. For this reason, the Fe–Cu system has been long studied as model to understand the basic mechanisms and the kinetic pathways leading to the formation of Cu precipitates and so called matrix damage in RPV steels, as well as the interaction of these features with dislocations, both experimentally [19–21] and by computer simulation [22–25]. It is important then to have a potential capable of reproducing in a reliable way both the solubility limit of Cu in Fe and the main features of point defects in the alloy.

Secondly, although two many-body Fe–Cu potentials are already available from the literature [5,6], neither of them appears to be fully suitable for radiation damage studies. As a matter of fact, it has been recently shown [10] that the reproduction of the thermodynamic properties of the Fe–Cu system using the potential proposed by Ackland et al. [5] (henceforth denoted as AB) is poor, in particular the solubility limit of Cu in Fe is about one order of magnitude higher than in reality. On the other hand, the potential developed by Ludwig et al. [6] (LF from now on), although reasonable from the thermodynamic point of view [26], exhibits a number of shortcomings concerning point defect description and interaction with Cu atoms. These are expected

to affect both the correct prediction of the configuration of Cu–V (V = vacancy) clusters [27], which are known to be formed during irradiation from positron annihilation experiments [20], and the kinetics of Cu precipitation [4]. In addition, recent kinetic MC studies have shown that the energy barriers for vacancy migration predicted by both potentials cannot reproduce the vacancy dragging effect observed using *ab initio* data [28] for the same barriers [29,30]. The actual existence of this effect is supported by the formation in irradiated Fe–Cu alloys of hollow Cu precipitates [20], suggesting that the fluxes of the two migrating species, vacancies and Cu atoms, should be in the same direction.

In summary, a technique based on the Ising formalism and the CVM theory, combined with the embedded atom method (EAM) for interatomic potentials [31], is developed in order to express analytically the thermodynamic functions of a substitutional alloy, aiming at optimizing the potential parameters so as to reproduce as closely as possible the corresponding phase diagram. The method is subsequently applied to the Fe–Cu system, due to the importance of this alloy for the understanding of the processes leading RPV steels to embrittlement during operation. Section 2 succinctly reviews the thermodynamic approach being pursued, its insertion in our fitting procedure, and more specific aspects of the method regarding the Fe–Cu system; Section 3 presents the newly derived potential including comparisons with previous models and with experiments; Section 4 discusses limitations, finer details, and possible improvements of the current methodology; finally, Section 5 summarizes our main conclusions.

2. Method

Only the main ideas are presented here, additional indications can be found in [32], whereas a more detailed account will be published elsewhere. According to general statistical mechanics principles, free energies can be expressed as variational problems in a configuration (site occupation) space [11,13]. Particularly, for rigid periodic lattices the Helmholtz free energy *per site*, $f(T,v,c)$, may be written as

$$f = \min_{\xi}\left\{\sum_{\alpha\subseteq\alpha_M} m_\alpha E_\alpha \xi_\alpha + k_B T \sum_{\alpha\subseteq\alpha_M} m_\alpha a_\alpha \sum_\sigma p_\alpha(\sigma)\ln p_\alpha(\sigma)\right\}, \tag{1}$$

where the first term represents the internal energy and the second one embodies the (configurational) entropy. The outer sums extend over the symmetry-equivalent clusters of sites, that are subsets of a (family of) chosen maximal ones, α_M. The multiplicity of these clusters is m_α; a_α are coefficients related to crystal symmetry and computed within the framework of the CVM theory; p_α are cluster probability distribution functions depending on the system configuration σ; the variational parameters ξ_α are the so called correlation functions, in turn linearly related to p_α; finally, E_α are the coefficients of the energy expansion upon the cluster basis used, thus carrying the specific interaction model. The latter is presently chosen to be in an EAM form [31]. We recall that according to this scheme the total energy is a sum of atomic/site contributions, that for a binary alloy can be expressed as

$$\begin{aligned} e_i &= \frac{1}{2}\sum_{j\neq i} V(t_i t_j; r_{ij}) + F(t_i;\rho_i),\\ \rho_i &= \sum_{j\neq i}\phi(t_i t_j; r_{ij}), \end{aligned} \tag{2}$$

where $t_i(t_j)$ stands for the chemical species at site $i(j)$, V are pair-like interaction terms, and F are the so called embedding functions that depend on the (heuristically) local electron density, ρ, which in turn results from the superposition of electronic potentials, ϕ. We take $\phi(t_i t_j; r) = \chi(t_i t_j)\psi(t_j; r)$ with $\chi(\mathrm{AA}) = \chi(\mathrm{BB}) = 1$, $\chi(\mathrm{AB}) = 1/\chi(\mathrm{BA}) = \chi$, and ψ the pure species electronic potentials. Parameter χ can then be interpreted as the relative strength among the pure species electronic potentials (when normalized to unit density). To carry out the energy expansion that appears in Eq. (1), we resort to the cluster probabilities, p_α, and make the approximation of retaining interactions up to three-body, i.e. the lowest many-body order. Regarding the entropy term, many calculations of phase diagrams using the CVM have been performed with relatively small α_M clusters, which nevertheless were able to obtain rather non trivial phase diagram structures. These are mainly the tetrahedron–octahedron approximation for the fcc lattices, and the tetrahedron approximation for bcc ones, which are used here in their expressions for disordered alloys [13].

The current fitting procedure considers $V(AA;r)$, $V(BB;r)$, $F(A;\rho)$, and $F(B;\rho)$ as given from the pure elements; the only unknown function is then the cross-pair interaction $V(AB;r)$ which contains the fitting parameters, $\{a_i\}$. This is given the common

form of a piece-wise cubic polynomial possessing some n_k knots at (chosen) positions r_i,

$$V(AB;r) = \sum_i^{n_k} a_i H(r_i - r)(r_i - r)^3, \quad (3)$$

where $H(x)$ is the Heaviside unit step. All potentials are imposed to reach up to the 5th neighbors shell, implying a host of three-body terms to be dealt with. Their number is however reduced by application of conditional probability concepts, resulting in a total of 13/10 independent correlation functions for the bcc/fcc lattice. The only remaining fitting parameter, χ, is currently fixed to an educated guess, guided e.g. by Miedema's semi-empirical n_{WS} scale [33].

Our general fitting strategy uses the fact that most properties we aim at fitting are linearly related to the energy. Then, the problem of matching the potential function to a given data set (from experiment, other calculations, etc.) can be cast as one of minimizing the overall squared deviation, so called objective function (OF), between linear expressions in the potential parameters and the associated data, possibly also imposing certain constraints. This may erroneously suggest that the current scheme is a quadratic programming problem; but it is not. Each data point of the phase diagram (T, c_α, c_β), representing equilibrium at temperature T between phases α and β of respective solute concentrations c_α and c_β, enters the OF through a couple of terms stemming form the common tangent construction. This implies a dependence of the OF on the correlation functions $\boldsymbol{\xi}$ that, through Eq. (1), are implicit functions of the potential parameters. The scheme is then highly nonlinear in the latter variables and can be envisaged as two nested minimizations: The inner one embodied in Eq. (1), that seeks to obtain the thermodynamic potential at fixed interaction parameters $\{a_i\}$, and the outer one that varies them in order to minimize the OF.

Two pieces of thermodynamic information were used to build up the OF for the current system, namely the mixing enthalpy for the Fe–Cu bcc phase as a function of concentration (10 points about evenly spaced) from Calphad calculations [34], taken as the excess energy per atom at 0 K for a random alloy, and the maximum solubilities of Cu and Fe at equilibrium in the coexisting bcc $\leftrightarrow$ fcc phases of the experimental Fe–Cu diagram [35] ($T \approx 1123$ K, 1.9 and 1.3 at% respectively). The rest of the physical input enters through constraints described next.

Firstly, the lattice parameters of the bcc random alloys contributing to the OF must be at equilibrium; this is translated as the requirement of null average pressure for each concentration point.

Secondly, as already mentioned, the Cu–V and Cu–Cu bindings are deemed to be important in determining the kinetics of Cu precipitation in Fe. Thus, control over Cu–V (1 nn and 2 nn, nn = nearest neighbor) and Cu–Cu (1 nn, 2 nn, and 3 nn) binding is exerted through approximate equations that neglect relaxation effects, the respective data being taken from *ab initio* calculations [28].

Thirdly, in order for the vacancy dragging of Cu atoms to occur, phenomenological models of transport coefficients [36,37] imply that the energy barriers leading to Cu–V (1 nn) and Cu–V (2 nn) configurations must be lower than the competing ones, leading to the dissociation of the complex. Thus, all the relevant barriers, as identified in Le Claire's model [38], were assessed through approximate equations based on a broken bond analysis and the condition that the vacancy exchange between 1 nn and 2 nn of the Cu atom should be easier than competing processes was imposed.

Lastly, *ab initio* calculations show that the mixed Fe–Cu $\langle 1\,1\,0\rangle$ dumbbell in the Fe matrix is unstable, while a weak attractive interaction may exist between the Fe–Fe $\langle 1\,1\,0\rangle$ dumbbell and a 1 nn Cu atom, located in the tensile-strained region of the dumbbell deformation field [39]. An attempt was made to approach this situation by adding a couple of splines to the pair potential in the region below 1 nn distance. This allows the repulsive part to be stiffened or softened until direct simulation suggests that an optimum has been reached.

3. Results

As mentioned, all the effort is put here in the fabrication of the cross potential. For the pure elements, two existing recent EAM potentials taken from the literature and considered to be among the most sophisticated according to current knowledge are selected. Namely the potential proposed by Mendelev et al. [40] for pure Fe and the one by Mishin et al. [41] for pure Cu, respectively named 'potential 2' and 'EAM1' in the original references. The electronic potentials from those sources were rescaled for convenience in such a way that, for both pure species, $\rho = 1$ in the reference state. Given the interpretation of the χ factor, this reference state was chosen to be the bcc structure for both

elements, at their respective equilibrium lattice parameters (Cu: 0.28683 nm, Fe: 0.28553 nm).

A series of cross potentials have been produced using the above overviewed fitting procedure; the latest one, denoted as CO5.20, is most likely among the best results possible within the EAM approach, compatible with the pure element potentials and for the application of interest. The pair terms are drawn in Fig. 1 in the effective gauge representation [42] for the pure elements. The cross-pair interaction has been obtained using 14 nodes in Eq. (3) evenly spaced between 0.235 and 0.550 nm, the respective parameters are reported in Table 2; the χ parameter was set to 1.59. It should be noted that the potential has not yet been adapted for a consistent handling of the very short distances, so that in its present form it might not be suitable for collision cascade simulations.

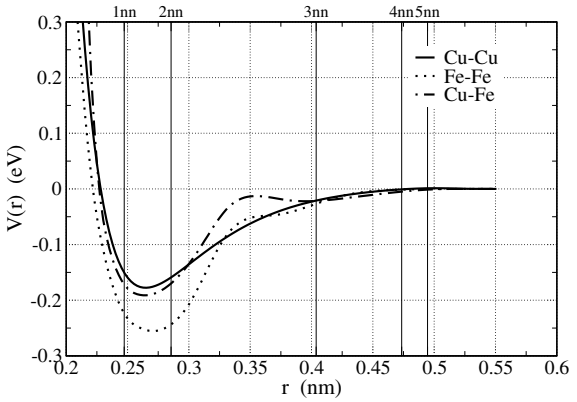

Fig. 1. Alloy pair potentials. Representation corresponds to the pure elements in the effective potential gauge. Neighbor shell positions in the Fe matrix indicated.

Table 2
Cross-pair potential coefficients, a_i (eV/nm^3), and knots, r_i (nm), in Eq. (3)

i	a_i	r_i
1	$0.1460151448E+01$	0.5500000000
2	$-0.4957562851E+02$	0.5257692308
3	$0.6998305005E+02$	0.5015384615
4	$-0.3874280553E+01$	0.4773076923
5	$-0.8723411300E+01$	0.4530769231
6	$0.6496879404E+02$	0.4288461538
7	$0.3695651396E+01$	0.4046153846
8	$-0.5082318050E+03$	0.3803846154
9	$-0.3076315854E+03$	0.3561538462
10	$0.2117344729E+04$	0.3319230769
11	$-0.1203932506E+04$	0.3076923077
12	$0.8046491939E+01$	0.2834615385
13	$0.2703349799E+04$	0.2592307692
14	$0.4000000000E+05$	0.2350000000

In Table 3 and Fig. 2 a number of binding energies of Cu–V complexes have been calculated with CO5.20 and compared to *ab initio* data. For completeness, the corresponding values predicted by the widely used LF and AB potentials are also included. Though the predictions of CO5.20 are not coincident with the *ab initio* ones, they represent a significant improvement over previous potentials. In particular, the existence of a 2 nn interaction is more correctly allowed for by CO5.20, although it turned out that trying to reproduce a Cu–V binding at 2 nn larger than at 1 nn gives rise to insurmountable inconsistencies. Overall, the sum of the squared differences between *ab initio* and potential predictions is reduced by a factor of two in going from LF or AB to CO5.20 ($\approx$0.2 eV^2 in the case of the former two, $\approx$0.1 eV^2 for the latter).

In Table 4 the main jump barriers according to Le Claire's model [38], depicted in Fig. 3, have been computed using AB, LF, and CO5.20, and again compared to *ab initio* results. It is seen that the values obtained with CO5.20 are closer to the latter than those produced by LF or AB: The overall squared deviation is decreased from $\approx$0.35 eV^2 (AB) or $\approx$0.25 eV^2 (LF) to $\approx$0.06 eV^2 (CO5.20). However, in order to fully grasp up to what extent this can make a relevant difference, the values were introduced in an atomistic kinetic MC (AKMC) code on barriers [30]. In AKMC simulations, atoms of both chemical species are located on a rigid lattice and the system evolves through exchanges between atoms and vacancies, simulating diffusion processes [22,43–45]. The input for the model are the vacancy migration barriers as functions of the local atomic configuration (i.e. type of jump), which are used to assess the jump frequency, decide the jump probability and choose the event according to the Monte Carlo scheme, thereby setting the rate of time employing a residence time algorithm [46]. Such an approach is similar to the one used by

Table 3
Ab initio [28] defect-pair binding energies (eV) compared to calculations using potentials CO5.20, LF [6], and AB [5]

Defect-pair	*Ab initio*	CO5.20	LF	AB
Cu–V (1 nn)	0.17	0.10	0.19	0.09
Cu–V (2 nn)	0.28	0.09	−0.03	0.04
Cu–Cu (1 nn)	0.14	0.08	0.19	0.08
Cu–Cu (2 nn)	0.04	0.08	−0.02	0.04

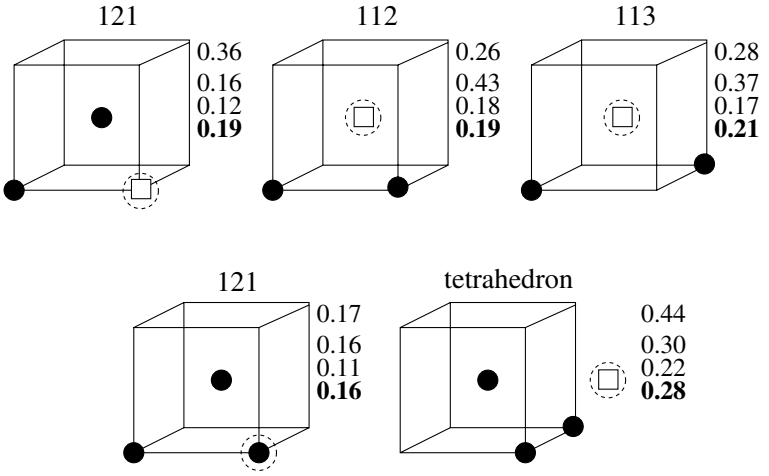

Fig. 2. Binding energies of vacancies (squares) and Cu atoms (black circles) for different defect agglomerates. The numbers, from top to bottom, correspond to *ab initio* [28], LF [6], AB [5], and CO5.20. The dashed circle encloses the object whose binding energy is given.

Table 4
Ab initio [28,56] energy barriers (eV) for the vacancy jumps of Fig. (3) compared to calculations using potentials CO5.20, LF, and AB

Jump designation	*Ab initio*	CO5.20	LF	AB
W_0(self-mig.)	0.64	0.63	0.68	0.78
W_2(exch.)	0.56	0.59	0.22	0.60
W_3(1 nn → 2 nn)	0.60	0.65	0.90	0.85
W'_3(1 nn → 3 nn)	0.65	0.71	0.66	0.83
W''_3(1 nn → 5 nn)	0.59	0.68	0.62	0.80
W_4(2 nn → 1 nn)	0.64	0.64	0.70	0.80
W'_4(3 nn → 1 nn)	0.50	0.62	0.47	0.74
W''_4(5 nn → 1 nn)	0.46	0.59	0.46	0.71
W_5(2 nn → 4 nn)	0.78	0.67	0.64	0.79
W_6(4 nn → 2 nn)	0.54	0.58	0.67	0.75

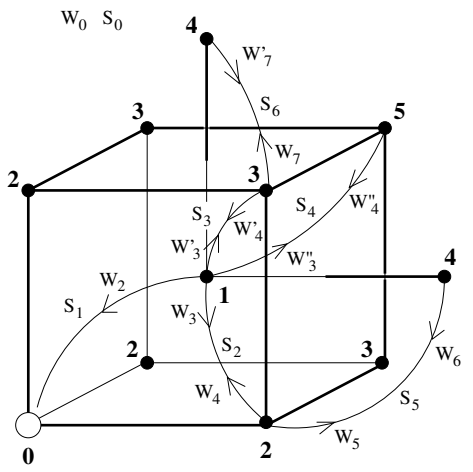

Fig. 3. Vacancy jumps (arrows) considered for the Cu–V dragging. Cu atom is at site 0. S_i stand for the approximate locations of the jumping atom.

Arokiam et al. [29]. It was thereby verified that the predicted CO5.20 barriers effectively allow the dragging of the Cu atom, in agreement with the use of *ab initio* barriers. This does not happen at all for the barriers computed with previous interatomic potentials: either the elements of the Cu–V pair keep exchanging positions until the pair splits (LF) or the pair has a negligible lifetime and the displacement of the two elements is always opposite (AB). Using the same technique it was also verified that the CO5.20 barriers provide essentially the same jump frequency and diffusion coefficient versus temperature for the Cu–V pair as *ab initio* barriers. The lifetime of the pair is somewhat shorter and the mean free path definitely shorter, but a dragging effect clearly exists. All this is illustrated in Fig. 4.

To conclude the description of point defects in Fe–Cu given by CO5.20, Table 5 compares the binding energy of a Cu atom to the Fe self-interstitial against *ab initio* [39] results for the different potentials considered here. It can be seen that CO5.20 reproduces very well the instability of the mixed Fe–Cu dumbbell, whereas the other potentials behave poorly in this respect. However, it was not possible to reproduce with the same fitting of CO5.20 also the relatively weak, attractive interaction with a 1 nn Cu atom located in the expanded region of the dumbbell strain field.

We turn now to the central aspect of our approach, i.e. to the validation of the thermodynamic properties as predicted by CO5.20, specifically the Cu solubility in the Fe matrix versus temperature. Two methods have been employed

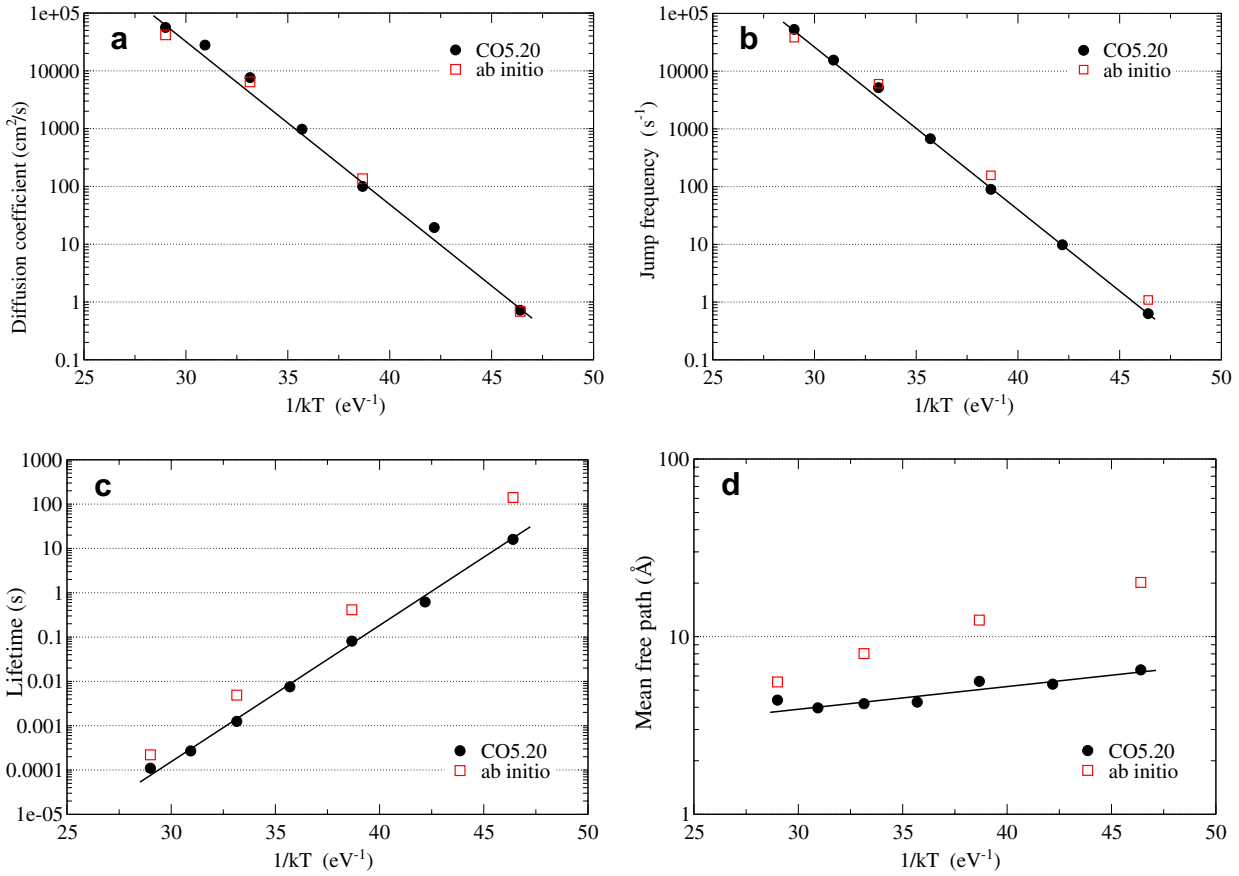

Fig. 4. (a) Diffusion coefficient, (b) jump frequency, (c) lifetime, and (d) mean free path, of the Cu–V pair vs. temperature calculated using the technique of atomistic kinetic MC on barriers. The barriers are from CO5.20 and *ab initio* [28,56] as indicated.

Table 5
Binding energies (eV) of Cu atoms to Fe–Fe dumbbells; *ab initio* values from [39]

Configuration	*Ab initio*	CO5.20	LF	AB
Fe–Cu ⟨110⟩ dum.	−0.43	−0.45	0.07	−0.08
Fe–Fe ⟨110⟩ dum. + 1 nn Cu	0.10	−0.03	0.09	0.02

for such a purpose, namely, Metropolis MC [47,48] (MMC) and a more sophisticated MC method implemented in the Alloy Theoretic Automated Toolkit package [49] (ATAT, freely available). The former can only provide the coexistence solubility curves corresponding to the equilibrium between a bcc-Fe-rich phase and a bcc-Cu-rich phase, while the latter can describe the (experimentally found) equilibrium between the bcc and the fcc phases of the Fe–Cu system. Both methods were applied in the rigid lattice approximation, which seems well justified for the present system. As a matter of fact, the results of using the ATAT package with the AB potential were compared with the curves from the complete phase diagram computed using full integration methods [10], without finding significant differences. This suggests that, for the considered system at least, the vibrational contributions to phase stability can be neglected.

Fig. 5 compares the results of the MMC calculations in the bcc phase performed with the three potentials. Since it is known that the structure of Cu precipitates of radius below about 4 nm is bcc [50], the figure is relevant to the initial stages of the precipitation and close to an actual simulation aimed at predicting its evolution. In this sense, the thermodynamic forces stemming from CO5.20 and LF are suggested to be very similar; however, from the above analysis of the barriers, the kinetic behavior will certainly be different, and so the respective predicted evolutions.

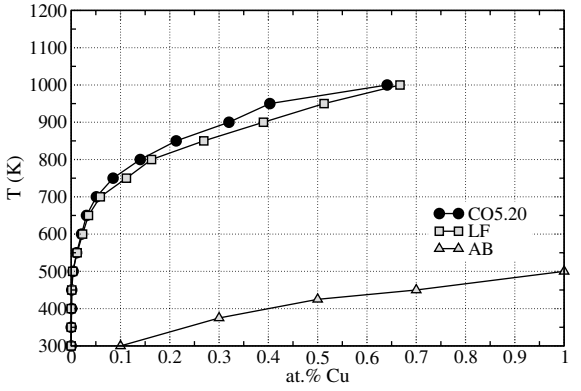

Fig. 5. Solubility limit of Cu in the Fe matrix calculated for the bcc phase by using the MMC technique and for the three potentials, CO5.20, LF, and AB, as indicated in the legend.

Fig. 6 shows the Cu solubility for the true thermodynamic phases in equilibrium, namely bcc and fcc. Also included are the experimental data from Salje and Feller-Kniepmeier [51] and from Perez et al. [52]. The former were obtained from the diffusion profile measurements of a thin Cu deposit onto an Fe substrate; the latter from thermoelectric power and small angle X-ray scattering measurements in thermally aged Fe–Cu alloys, where precipitation was thereby induced. In fact, the latter points correspond to Eq. (10) of Perez et al. [52] evaluated at the measuring temperatures. Clearly, CO5.20 follows the experimental results very reasonably, perhaps with a little over/under-estimated solubilities for temperatures below/above 1000 K, the other two potentials giving too high solubilities, particularly AB, as anticipated.

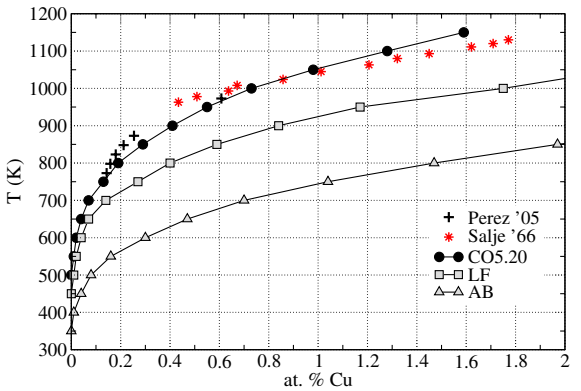

Fig. 6. Solubility limit of Cu in the Fe matrix for the thermodynamic equilibrium bcc ↔ fcc. Calculations were performed with the ATAT package [49] for the three potentials indicated. Experimental data are from Refs. [51,52].

4. Discussion

Fitting interatomic potentials consistent with a host of experimental or calculated data generally involves trading between conflicting aspects. Clearly those related to the intended range of applications receive the most attention, while compatibility with others is conditioned, at last, by the potential form itself, no matter how much flexibility (i.e. parameters) this form may possess. Since we wanted a tool as reliable as possible to study the long term microstructure evolution of Fe–Cu alloys under irradiation, the effort was mostly concentrated on the thermodynamic aspects, particularly the phase diagram, because they embody the driving forces governing such an evolution. On the other hand, some features related to point defects, though apparently better described than in existing empirical cohesive models, resulted less well represented, at least if we rely on density functional theory indications. This is the case for instance of the Cu–V and Cu–Cu bindings, where *ab initio* calculations predict a sizeably larger/smaller binding energy at 2 nn as compared to 1 nn respectively, neither of which could be captured by the present model. In this sense one should note that, though *ab initio* calculations are currently the most reliable technique to access this kind of defect properties, their accuracy in connection with energy differences of the order of tenths of eV may anyway be questioned. The choice made in the present work was to reach a certain level of acceptability versus *ab initio* calculations, without forcing a perfect agreement that may have jeopardized the performance of the potential on other aspects. More on the positive side, an important dynamical effect, such as the dragging of Cu atoms by vacancies, is at least qualitatively accounted for, a unique feature of the present potential. Regarding the thermodynamics, we have seen that the Cu solubility in the Fe matrix is predicted to be in fairly good agreement with experiment; also, even though not presently shown, atomistic simulations of random Fe–Cu alloys resulted in very good agreement for the mixing energy as compared to Calphad calculations [34]. Other aspects of the phase diagram such as the magnetic-induced transitions to the fcc phase on the Fe-rich side are beyond the reach of the bare EAM's interaction and their prediction outside the scope of the present work, as is accounting for the liquid phases beyond the reach of the CVM approach. Referring to the latter, we note that liquid-like configurations were

considered in the development of the Fe potential being used, and that the calculated melting points of 1772 K [40] and 1330 K [41] for Fe and Cu respectively, are in very reasonable agreement with experiment (1812 K and 1358 K). Qualitatively wrong equilibria between solid and liquid phases are therefore not expected.

Turning now to the methodology developed for the purpose of fitting the proposed potential, though its formulation is fairly straightforward, its practical application is by no means free of fine details. We have found that the precision with which the energy of arbitrary configurations is calculated via cluster expansion (within 1 meV) is a delicate issue for the reliable prediction of the phase diagram. In the present case the problem is not especially serious and consistent results for the solubility limit versus temperature have been obtained using different techniques (i.e. CVM, ATAT and also MMC). Generally, however, difficulties for the final validation may arise, as different tools to build the phase diagram may provide different results. Ways to improve the energy expansion are currently under investigation.

Another delicate point refers to the determination of the thermodynamic potential via minimization with respect to the correlation functions. Apparently, for relatively low temperatures and for concentrations approaching the pure phases, more than one minimum may exist and, when building the CVM phase diagram, the system may remain trapped for a while in non-physical extrema. The problem was alleviated by starting from high temperatures and cooling down in steps of 25–50 K, with the intention of continuously dragging the state deemed to be physically meaningful. In spite of these problems, evidence suggests that the method, possibly after further refinement, is robust enough to be applied in a generalized way to other alloys. Particularly, we tried to fit either to the mixing enthalpy only, or to the phase diagram point only. Consistently, we found that, although fitting to the mixing enthalpy curve may be enough to provide a reasonable thermodynamic behavior, fitting to the single phase diagram point is sufficient to have not only a good thermodynamic behavior, but also a reasonable mixing enthalpy curve.

The method needs now to be applied to other, more challenging systems, e.g. characterized by a larger solubility limit than Fe–Cu, for example Fe–Cr, where the mixing enthalpy curve also exhibits a change of sign [53], so that modifications of the EAM form must be used [54,55], or Fe–Ni, where intermetallic compounds make their appearance.

5. Summary and conclusions

A method to fit interatomic potentials for binary alloys using phase diagram data has been developed, based on the Ising formalism combined with the EAM expression for the energy and the cluster variation method for the entropy. The method has been applied for the construction of a new Fe–Cu interatomic potential, using for the pure elements rather sophisticated EAM potentials for Fe and Cu currently available in the open literature. In addition, *ab initio* results for Cu–V binding energies, vacancy migration barriers around a Cu atom and mixed dumbbell stability have been used as a guide for the fitting. This potential has been proven to reproduce very nicely the thermodynamic properties of the alloy known from experiments and to provide descriptions of the interaction between Cu atoms and point defects in Fe closer to *ab initio* indication than with other existing potentials. It is therefore believed that this potential is suitable for the study of the evolution kinetics under irradiation of Fe–Cu systems. More generally the applied methodology, which can be easily extended to modifications of the EAM form, seems robust enough to produce interatomic potentials for radiation damage studies consistent with thermodynamics for other relevant binary systems, such as Fe–Cr and Fe–Ni.

Acknowledgements

This work was performed in the framework of the PERFECT Integrated Project of the 6th Framework Programme, partly funded by the European Commission under contract F16O-CT-2003-508840. The work was also sponsored by the Belgian Scientific Policy Office, who promoted the bilateral agreement between SCK-CEN and CNEA, under contract CO 90 03 31662.00 (TANGO Project). R.P. acknowledges support from ANPCyT-PICT 1206164 and CONICET-PICT 5062. Thanks also to Drs H. Mosca and P. Alonso for fruitful discussions on CVM, to Dr F. Djurabekova for providing the barrier calculations and relevant AKMC results, to Mr G. Bonny for his criticisms, to Dr M. Powell for making his COBYLA code freely available, and to the Harwell subroutine library for providing free versions of some of their routines. Last but not least, thanks to the international community of free software developers.

References

[1] S.M. Foiles, M.I. Baskes, M.S. Daw, Phys. Rev. B 33 (12) (1986) 7983.
[2] A.F. Voter, S.P. Chen, Mater. Res. Soc. Symp. Proc., Vol. 82, MRS, Pittsburg, Pennsylvania, 1987, p. 175.
[3] G.J. Ackland, V. Vitek, Phys. Rev. B 41 (15) (1990) 10324.
[4] Y.N. Osetsky, A. Serra, Philos. Mag. A 73 (1) (1996) 249.
[5] G.J. Ackland, D.J. Bacon, A.F. Calder, T. Harry, Philos. Mag. A 75 (3) (1997) 713.
[6] M. Ludwig, D. Farkas, D. Pedraza, S. Schmauder, Modelling Simul. Mater. Sci. Eng. 6 (1998) 19.
[7] D. Frenkel, B. Smit, Understanding molecular simulation, 2nd Ed., Computational Science Series, vol. 1, Academic, 2002.
[8] D.A. Kofke, E.D. Glandt, Mol. Phys. 64 (1988) 1105.
[9] E. Ogando Arregui, M. Caro, A. Caro, Phys. Rev. B 66 (5) (2002) 54201.
[10] E.M. Lopasso, M. Caro, A. Caro, P. Turchi, Phys. Rev. B 68 (21) (2003) 214205.
[11] F. Ducastelle, Order and phase stability in alloys, Cohesion and structure, vol. 3, North-Holland, 1991.
[12] R. Kikuchi, Phys. Rev. 81 (6) (1951) 988.
[13] G. Inden, W. Pitsch, Atomic ordering, in: R.W. Cahn, P. Haasen, C.J. Kramer (Eds.), Phase Transformations in Materials, Materials Science and Technology, vol. 5, John Wiley & Sons, Weinheim, 1991, Chapter 9, p. 497.
[14] G. Odette, Scr. Metall. 17 (1983) 1183.
[15] W. Phythian, C. English, J. Nucl. Mater. 205 (1993) 162.
[16] C. English, W. Phythian, R. McElroy, Mater. Res. Soc. Symp. Proc., vol. 439, MRS, Pittsburg, Pennsylvania, 1997, p. 471.
[17] G. Odette, G. Lucas, JOM 53 (7) (2001) 18.
[18] R. Chaouadi, R. Gérard, J. Nucl. Mater. 345 (2005) 65.
[19] P. Auger, P. Pareige, A. Akamatsu, D. Blavette, J. Nucl. Mater. 225 (1995) 225.
[20] Y. Nagai, Z. Tang, M. Hassegawa, T. Kanai, M. Saneyasu, Phys. Rev. B 63 (13) (2001) 134110.
[21] K. Morita, S. Ishino, T. Tobita, Y. Chimi, N. Ishikawa, A. Iwase, J. Nucl. Mater. 304 (2002) 153.
[22] F. Soisson, A. Barbu, G. Martin, Acta Mater. 44 (1996) 3789.
[23] J. Blackstock, G. Ackland, Philos. Mag. A 81 (9) (2001) 2127.
[24] C. Domain, C. Becquart, L. Malerba, J. Nucl. Mater. 335 (2004) 121.
[25] D. Bacon, Y. Osetsky, J. Nucl. Mater. 329 (2004) 1233.
[26] A. Caro, M. Caro, E. Lopasso, P. Turchi, D. Farkas, J. Nucl. Mater. 349 (2006) 317.
[27] D. Kulikov, L. Malerba, M. Hou, Philos. Mag. 86 (2) (2006) 141.
[28] C.S. Becquart, C. Domain, Nucl. Instrum. and Meth. B 202 (2003) 44.
[29] A.C. Arokiam, A.V. Barashev, D.J. Bacon, in: N.M. Ghoniem (Ed.), 2nd Int. Conf. on Multiscale Materials Modeling, Mechanical and Aerospace Engineering Dept., UCLA, 2004, p. 480.
[30] F.G. Djurabekova, L. Malerba, C. Domain, C.S. Becquart, in: Proc. 8th Int. Conf. on Computer Simulation of Radiation Effects in Solids (COSIRES 2006), Richland, Washington, USA, June 18–23, 2006, Nucl. Instrum. and Meth. B., accepted for publication.
[31] M.S. Daw, M.I. Baskes, Phys. Rev. B 29 (12) (1984) 6443.
[32] L. Malerba, R.C. Pasianot, SCK-CEN Report ER-6, Feb. 2006.
[33] A.R. Miedema, Z. Metallkd. 70 (6) (1979) 345.
[34] A. Caro, P. Turchi, M. Caro, E.M. Lopasso, J. Nucl. Mater. 336 (2005) 233.
[35] T.B. Massalski (Ed.), Binary Alloy Phase Diagrams, 2nd Ed., ASM International, Metals Park, OH, 1990.
[36] Y. Okamura, A.R. Allnatt, J. Phys. C: Solid State Phys. 16 (1983) 1841.
[37] Y. Serruys, G. Brebec, Philos. Mag. A 46 (4) (1982) 661.
[38] A.D. Le Claire, J. Nucl. Mater. 69&70 (1978) 70.
[39] C. Domain, C.S. Becquart, Phys. Rev. B 65 (2) (2001) 24103.
[40] M.I. Mendelev, A. Han, D.J. Srolovitz, G.J. Ackland, D.Y. Sun, M. Asta, Philos. Mag. A 83 (35) (2003) 3977.
[41] Y. Mishin, M.J. Mehl, D.A. Papaconstantopoulos, A.F. Voter, J.D. Kress, Phys. Rev. B 63 (22) (2001) 224106.
[42] M.W. Finnis, J.E. Sinclair, Philos. Mag. A 50 (1) (1984) 45.
[43] B. Wirth, G. Odette, Mater. Res. Soc. Symp. Proc., vol. 540, MRS, Pittsburg, Pennsylvania, 1999, p. 637.
[44] C. Domain, C. Becquart, J.C. Van Duysen, Mater. Res. Soc. Symp. Proc., vol. 540, MRS, Pittsburg, Pennsylvania, 1999, p. 643.
[45] L. Malerba, C. Becquart, M. Hou, C. Domain, Philos. Mag. 85 (4–7) (2005) 417.
[46] W. Young, E. Elcock, Proc. Phys. Soc. 89 (1966) 735.
[47] N. Metropolis, A. Rosenbluth, N. Rosenbluth, A. Teller, E. Teller, J. Chem. Phys. 21 (1953) 1087.
[48] O. Khrushcheva, E. Zhurkin, L. Malerba, C. Becquart, C. Domain, M. Hou, Nucl. Instrum. and Meth. B 202 (2003) 68.
[49] A. van de Walle, M. Asta, G. Ceder, CALPHAD 26 (2002) 539, <http://cms.northwestern.edu/atat>.
[50] R. Monzen, M. Jenkins, A. Sutton, Philos. Mag. A 80 (3) (2000) 711.
[51] G. Salje, M. Feller-Kniepmeier, J. Appl. Phys. 48 (5) (1977) 1833.
[52] M. Perez, F. Perrard, V. Massardier, X. Kebler, A. Deschamps, H. de Monestrol, P. Pareige, G. Covarel, Philos. Mag. 85 (20) (2005) 2197.
[53] P. Olsson, I. Abrikosov, L. Vitos, J. Wallenius, J. Nucl. Mater. 321 (2003) 84.
[54] A. Caro, D.A. Crowson, M. Caro, Phys. Rev. Lett. 95 (2005) 75702.
[55] P. Olsson, J. Wallenius, C. Domain, K. Nordlund, L. Malerba, Phys. Rev. B 72 (2005) 214119.
[56] C. Domain, private communication.